# Human Cathepsin B Is a Metastable Enzyme Stabilized by Specific Ionic Interactions Associated with the Active Site†

Boris Turk,*,‡ Iztok Dolenc, Eva Žerovnik, Dušan Turk, Franc Gubenšek, and Vito Turk

*Department of Biochemistry and Molecular Biology, J. Stefan Institute, Jamova 39, Ljubljana, Slovenia*

*Received June 20, 1994; Revised Manuscript Received September 12, 1994*®

ABSTRACT: The effect of neutral or alkaline pH on cathepsin B activity and structure was investigated. An irreversible loss of activity, accompanied by large structural changes, was observed at pH ≥7.0. The high activation energy of 183.5 kJ $mol^{-1}$, calculated for the inactivation process, is in good agreement with structural changes observed by circular dichroism. Both the pH-induced inactivation and the pH-induced unfolding of cathepsin B were found to be first-order processes, exponentially increasing with increasing pH of the solution. The good agreement of the rate constants of inactivation and unfolding of the enzyme indicates an important structure−function relationship. Cathepsin B was also found to be destablized both by increasing ionic strength and organic solvent content.

Cathepsin B is the most abundant and the most studied lysosomal cysteine proteinase. Beside its role in intracellular protein degradation (Barrett & Kirschke, 1981) it has been implicated in tumor metastasis (Sloane, 1990; Sloane et al., 1990; Moin et al., 1992) and other diseases such as arthritis and muscular dystrophy (Mort et al., 1984).

Cathepsin B exhibits optimal activity against most substrates in slightly acidic media (Barrett & Kirschke, 1981), while at pH values above 7.0 its activity falls sharply due to irreversible inactivation (Barrett, 1973). Cathepsin B acts both as endopeptidase and as dipeptidyl carboxypeptidase (Aronson & Barrett, 1978; Bond & Barrett, 1980). Although several studies have been made, the mechanism of its catalysis and specificity is still not well understood. Complex behavior with several dissociable groups involved was suggested from the pH−activity profiles (Bajkowski & Frankfater, 1983a,b; Willenbrock & Brocklehurst, 1985b, 1986; Polgar & Csoma 1987; Khouri et al., 1992; Hasnain et al., 1992, 1993). On the basis of these profiles, it was concluded that dissociation of the active-site thiol leads to the formation of an ion pair between Cys29 and His199, as in papain. Although several models have been proposed to explain the pH−activity profiles of cathepsin B (Willenbrock & Brocklehurst, 1984, 1985b, 1986; Polgar & Csoma, 1987; Khouri et al., 1992; Hasnain et al., 1992), they all agree that the enzyme is inactivated by deprotonation of the active-site His199. The crystal structure of human liver enzyme (Musil et al., 1991) has also shown several charged groups in the active−site region, but did not resolve the roles of all of them.

Our previous study on the pH-induced inactivation of human cathepsin L was the first detailed study made of this problem on any lysosomal cysteine proteinase (Turk et al., 1993a). Unfortunately, the crystal structure of cathepsin L, which could give more information about the mechanism of the process, is not known yet. In other studies on the pH-induced inactivation of cysteine proteinases, the process was only qualitatively described (Barrett, 1973; Machleidt et al., 1986; Willenbrock & Brocklehurst, 1985a; Khan et al., 1992) or little quantitative data were presented (Baici & Knöpfel 1986; Baici et al., 1988). Here we present a kinetic study of the irreversible pH-induced inactivation of human cathepsin B. Inactivation of the enzyme is shown to be accompanied by large structural changes and highly dependent on pH, temperature, and ionic strength of the medium.

## MATERIALS AND METHODS

Z-Arg-Arg-AMC[1] was purchased from Bachem (Bubbendorf, Switzerland), and dithiothreitol, papain (2× crystallized), and EDTA were from Sigma (St. Louis, MO). Sephacryl S-200 thiol Sepharose 4B, and an FPLC Mono S column were purchased from Pharmacia (Uppsala, Sweden). Iodoacetic acid and dimethyl sulfoxide were from Merck (Darmstadt, Germany). Stock solutions of substrates were prepared in dimethyl sulfoxide. Ep-475 was from the Peptide Research Institute (Osaka, Japan). All other chemicals used were of analytical grade. The protein concentration of cathepsin B was determined by absorption measurements, where an absorption coefficient = 1.8 L $g^{-1}$ $cm^{-1}$ (Zvonar et al., 1979) and $M_r$ = 28 000 (Barrett & Kirschke, 1981; Ritonja et al., 1985) were used.

Unless otherwise stated, all kinetic measurements were done in 50 mM Tris buffer of desired pH, containing 100 mM NaCl, 1 mM EDTA, and 0.5% (v/v) or less dimethyl sulfoxide at 37 °C.

*Purification of Human Spleen Cathepsin B.* Cathepsin B was purified from human spleen using a procedure similar to that previously described for the purification of cathepsin B from human liver (Zvonar et al., 1979). Prior to ammonium sulfate precipitation, the homogenate was incu-

† The work was supported by the Ministry of Science and Technology of the Republic of Slovenia. The manuscript was finished when B.T. was supported with a FEBS Fellowship.

* Corresponding author

‡ Present address: Department of Veterinary Medical Chemistry, Swedish University of Agricultural Sciences, Biomedical Center, Box 575, S-751 23 Uppsala, Sweden.

® Abstract published in *Advance ACS Abstracts,* November 1, 1994.

[1] Abbreviations: AMC, 4-methyl-7-coumarylamide; CPI, cysteine proteinase inhibitor; Ep-475, [2*S*-[2α,3β(*R**)]]-3-[[[3-methyl-1-[[(3-methylbutyl)amino]carbonyl]butyl]amino]carbonyl]oxiranecarboxylic acid; Z-, benzyloxycarbonyl. Enzymes: Papain (EC 3.4.22.2), cathepsin B (EC 3.4.22.1).

0006-2960/94/0433-14800$04.50/0 © 1994 American Chemical Society

bated for 2 h at 37 °C and pH 4.2. Fractionated ammonium sulfate precipitation was not a necessary step, since only a negligible amount of precipitate was formed between 0 and 30% of saturation. The precipitate obtained by 75% of saturation was dialyzed against 100 mM acetate buffer, pH 5.0, containing 300 mM NaCl and 2 mM EDTA. Insoluble proteins were removed by centrifugation. The sample was further purified by gel filtration on a Sephacryl S-200 column instead on Sephadex G-75. After the chromatography on thiol Sepharose 4B, thiol enzymes were dialyzed against 20 mM acetate buffer, pH 5.0, containing 1 mM EDTA. The dialyzed sample was then applied to an FPLC Mono S column equilibrated with the same buffer, which was used instead of a Cm-cellulose column. Bound proteins were eluted with a 0−0.25 M NaCl gradient in the starting buffer (flow rate of 1 mL/min) at room temperature. Cathepsin B eluted at 0.115 M NaCl. Afterward cathepsin B was active-site titrated with Ep-475 as described previously (Turk et al., 1993b). From 0.5 kg of human spleen we obtained about 1 mg of pure cathepsin B, which was highly active (>80%).

*Inactivation Kinetics of Cathepsin B.* Z-Arg-Arg-AMC of appropriate concentration (0.02−1 mM) was dissolved in 1.98 mL of Tris buffer. Cathepsin B was activated in the 0.1 M phosphate buffer, containing 1 mM EDTA and 5 mM dithiothreitol, pH 6.0, for 5 min and then the reaction was started by the addition of 20 μL of enzyme (final concentration 0.03−0.6 nM) to the reaction mixture. Progress of the reaction was followed by monitoring of the fluorescence of the released product in a thermostated Perkin-Elmer LS-3 spectrofluorimeter at excitation and emission wavelengths of 380 and 470 nm, respectively. The fluorimeter was on-line with an IBM XT microcomputer and controlled by Flusys software (Rawlings and Barrett, 1990). At least four or five experiments were done at each substrate or enzyme concentration. All the reactions were performed with less than 5% of substrate consumption unless otherwise stated.

When the inactivation was too slow to be measured as described above, a different method was used. Preactivated cathepsin B (40 μL) was added to 960 μL of thermostated buffer solution to a final concentration of 0.5 μM. After appropriate intervals, 50 μL aliquots were taken to test the residual activity using 200 μM Z-Arg-Arg-pNA as substrate in the 100 mM phosphate buffer, pH 6.0, containing 1 mM EDTA and 2 mM dithiothreitol. The progess of the reaction was followed for 30 s at 410 nm. Usually 10−15 data pairs (time, absorbance) were obtained in that way for each curve.

Faster reactions were monitored with a DX-17 MV stopped-flow apparatus (Applied Photophysics, UK). One syringe was filled with 20 μM Z-Arg-Arg-AMC dissolved in appropriate buffer, and the other one with cathepsin B, preactivated as described above. A 10:1 mixing ratio (v/v) was used to achieve the unchanged final pH of the reaction. The release of AMC was observed by monitoring of the fluorescence at excitation wavelength 360 nm through the cutoff filter with 50% transmission at ~400 nm. At least six or seven individual measurements were made at every pH value.

In the absence of substrate the unfolding was followed by measurement of the integrated fluorescence at excitation wavelength 285 nm and through the cutoff filter with 50% transmission at ~295 nm with a DX-17 MV stopped-flow apparatus as described above.

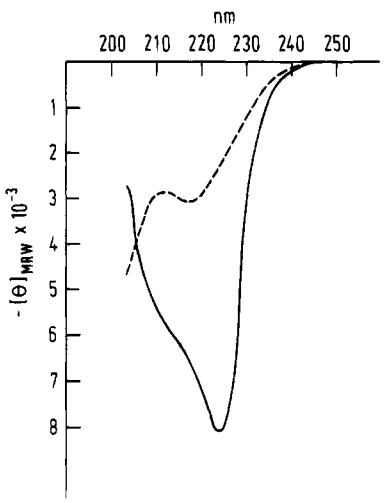


FIGURE 1: Far UV (205−245 nm) circular dichroism spectra of cathepsin B at pH = 5.5 (solid line) and at pH = 7.4 (dashed line). Experimental conditions were as described under Materials and Methods. The CONTIN analyses of both spectra are given below; the values are listed solely for the comparison of both states. *R*, remainder. *From the crystal structure of human cathepsin B (Musil et al., 1991).

| pH | α-helix (%) | β-sheet (%) | R (%) |
|---|---|---|---|
| | 27* | 23* | 50* |
| 5.5 | 34 | 22 | 44 |
| 7.4 | 2 | 47 | 51 |

Reversibility of cathepsin B inactivation was studied as described previously for cathepsin L (Turk et al., 1993a), except that cathepsin B was incubated at pH 7.4 for 3 h and that reactivation was studied in 100 mM phosphate buffer, containing 1 mM EDTA, pH 6.0.

*Circular Dichroism Measurements.* Circular dichroism in the near (260−320 nm) and far (205−245 nm) ultraviolet regions was measured by a Dichrograph III (Jobin Yvon, France) at 20 °C and at pH 5.5 and 7.4. Cells of 1 cm pathlength for the near UV and 0.1 cm for the far UV were used. After the measurement at pH 5.5, cathepsin B was dialyzed overnight against 100 mM Tris buffer, pH 7.4, and incubated for 3 h at 37 °C, followed by the measurement at pH 7.4. The mean residue ellipticity in deg $cm^2$/dmol was calculated using a mean weight of 112/residue (MRW). Structural changes were also followed continuously by the measurement of circular dichroism at 222 nm as follows: 15 μL of cathepsin B, dissolved in 20 mM acetate buffer, pH 5.5, containing 1 mM EDTA (0.5 μM final concentration), was mixed with 165 μL of thermostated buffer (Tris or 50 mM Hepes, containing 1 mM EDTA and 100 mM NaCl) and placed into a 0.1 cm cuvette, after which the progress of the unfolding was observed.

## RESULTS

*Circular Dichroism Spectra.* The far UV circular dichroism spectra of cathepsin B at pH 5.5 and 7.4 are shown in Figure 1. As can be seen, the minimum at 222 nm at pH 5.5 is shifted to 218 nm at pH 7.4. Both spectra have been analyzed using the CONTIN method (Provencher, 1982; Provencher & Glöckner, 1981) and the fractions of α and β and the remainder (*R*) secondary structure are gathered and compared to the crystallographic data in the legend to Figure 1. A dramatic decrease in the α-helix content is detected at pH 7.4, whereas the β-sheet content apparently increases.

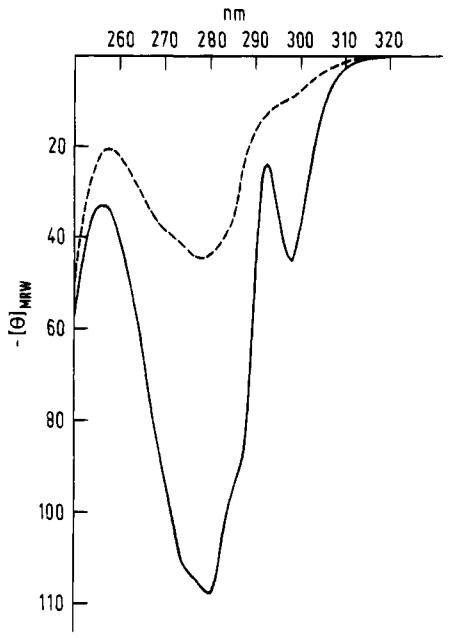


FIGURE 2: Near UV (260−320 nm) circular dichroism spectra of cathepsin B at pH = 5.5 (solid line) and at pH = 7.4 (dashed line). Other experimental details were as described under Materials and Methods.

However, the results should only be taken as approximate, since the data were collected only to 205 nm.

Large differences between circular dichroism spectra at the tested pH values have also been observed in the near UV region (Figure 2). The peak with a minimum at 298 nm, corresponding to tryptophan residues, has disappeared. Also the intensity of the peak with minimum at 280 nm is lowered by a factor of 3.

*Inactivation Kinetics of Cathepsin B.* The kinetics of the pH-induced inactivation of cathepsin B was studied at pH ≥ 7.0 and the reaction between cathepsin B and the substrate (Z-Arg-Arg-AMC) was monitored continuously. All progress curves obtained were exponential, and could be best fitted to the following first-order relationship (Tian & Tsou, 1982):

$$P = P_\infty(1 - e^{-k_{obs}t}) \quad (1)$$

where $P$ and $P_\infty$ are the product concentration at a given or infinite time, respectively, and $k_{obs}$ is the observed first-order inactivation rate constant. At pH ≥ 8.5, substantial spontaneous substrate degradation was observed during the reaction. The progress curves obtained in the pH range 8.5−9.5 were therefore fitted to the following modified eq 1 (Cha, 1975; Morrison & Walsh, 1988; Figure 3):

$$P = P_\infty(1 - e^{-k_{obs}t}) + v_{sd}t \quad (2)$$

where $v_{sd}$ represents the rate of spontaneous substrate degradation. Slow reactions, which were carried out in the absence of substrate and monitored by pouring aliquots of the reaction medium into substrate, were also fitted to the first-order rate equation.

The effect of enzyme concentration on the rate of inactivation was studied at 37 °C at pH 8.0 and 9.5, using 20 μM Z-Arg-Arg-AMC as a substrate. The inactivation rate was found to be independent of the enzyme concentration in the range studied (0.03−5 nM at pH = 8.0; 50−500 nM at pH 9.5) and of the substrate concentration between

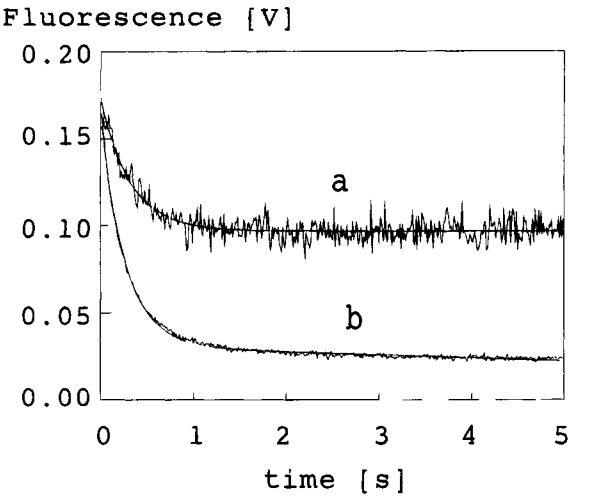


FIGURE 3: Progress curves for unfolding (a) and inactivation (b) of human cathepsin B at pH 9.5 and at 37 °C. The reaction media contained 400 nM cathepsin B (final concentration) (a) or 150 nM cathepsin B, 20 μM Z-Arg-Arg-AMC, and 0.5% (v/v) of dimethyl sulfoxide (b). Other experimental details were as described under Materials and Methods. The solid lines crossing the stopped-flow traces are the theoretical single-exponential curves generated using eq 1 (a) and the best estimate of $k_{unf}$, and eq 2 (b) and the best estimates of $k_{obs}$ and $v_{sd}$, calculated by nonlinear regression analysis.

20 μM and 1 mM Z-Arg-Arg-AMC at pH = 8.0 and 37 °C. In an attempt to compare rates of the inactivation and of unfolding the latter was also followed by the continuous measurement of circular dichroism at 222 nm as described in the Materials and Methods section. Circular dichroism decreased exponentially (not shown). This decrease could be described by the following equation:

$$E = E_0 e^{-k_{unf}t} \quad (3)$$

where $E$ and $E_0$ represent circular dichroism at a given time and time zero, respectively, and $k_{unf}$ is the observed first-order rate constant for the unfolding of the enzyme. The rate constants obtained in this way were similar to the inactivation rate constants ($k_{inac} = 1.38 \times 10^{-3}$ s$^{-1}$ and $k_{unf} = 1.45 \times 10^{-3}$ s$^{-1}$ at pH = 8.0 and 25 °C; Table 1), thus suggesting that both processes might be linked. The conformational changes of cathepsin B could also be followed by the continuous measurement of intrinsic fluorescence. The experimental curves were fitted to eq 1 (Figure 3a). $P$ and $P_\infty$ represent the fluorescence at a given time and the fluorescence at infinite time, respectively, and $k_{obs}$ is the observed unfolding rate constant. Attempts to fit the experimental unfolding curves to double exponentials resulted in two closely spaced values, but did not improve the $\chi^2$ error. The rate constants for the unfolding of the enzyme, measured by fluorescence changes, were independent of enzyme concentration and were very similar to the values of inactivation rate constants (Table 1), supporting the above conclusion.

*Effect of pH, Ionic Strength, and Temperature on the Inactivation Rate Constant, $k_{inac}$.* The inactivation of cathepsin B was studied in the pH range 7.0−9.5 at 37 °C. At pH = 7.0, 50 mM phosphate buffer, containing 100 mM NaCl and 1 mM EDTA, was used. In the pH range 7.5−8.5, Tris buffer was used while at pH = 8.8−9.5 the reaction buffer consisted of 50 mM glycine−NaOH, 100 mM NaCl, and 1 mM EDTA. Table 1 shows that the rate of inactivation is

Table 1: Effect of pH on the Rate of Inactivation of Cathepsin B at 37 °C[a]

| pH | $10^3 \times k_{obs}$ ($s^{-1}$) | $t_{1/2}$ (s) | $10^3 \times k_{obs}$ ($s^{-1}$) | $t_{1/2}$ (s) | $10^3 \times k_{obs}$ ($s^{-1}$) | $t_{1/2}$ (s) |
|---|---|---|---|---|---|---|
| 7.00 | 0.54 ± 0.06[b] | 1281 | ND | | 0.75 ± 0.04[d] | 924 |
| 7.50 | 1.23 ± 0.17 | 563 | ND | | ND | |
| 8.00 | 8.5 ± 1.0 | 81 | ND | | ND | |
| 8.50 | 74.6 ± 5.2 | 9.3 | ND | | ND | |
| 8.80 | 500 ± 39 | 1.4 | 273 ± 11[c] | 2.5 | ND | |
| 9.00 | 812 ± 56 | 0.85 | ND | | 1030 ± 65[e] | 0.67 |
| 9.50 | 3750 ± 278 | 0.18 | 2247 ± 152[c] | 0.31 | 3130 ± 185[e] | 0.22 |

[a] The best estimates for the observed inactivation rate constant, $k_{obs}$, are given together with their standard errors obtained by nonlinear regression analysis. Corresponding half-lives were calculated using the following relationship: $t_{1/2} = \ln 2/k_{obs}$. Inactivation of cathepsin B was observed in the presence of 20 μM Z-Arg-Arg-AMC, other experimental conditions were as described under Materials and Methods. [b] Determined in the absence of substrate by a discontinuous method. [c] Rate constants in the absence of NaCl. [d] Unfolding rate constant measured by circular dichroism. [e] Unfolding rate constants measured by stopped-flow fluorimetry. ND = not determined.

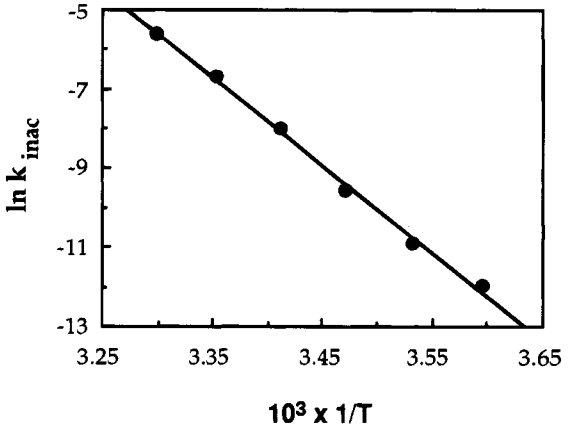


FIGURE 4: Arrhenius plot for the first-order rate constant, $k_{inac}$, at pH = 8.0. The $k_{inac}$ values were calculated using eq 3. The solid line is the best fit, calculated by linear regression analysis.

remarkably sensitive to pH. The process, which is quite a slow one at pH = 7.0 ($k_{obs} = 5.41 \times 10^{-4}$ $s^{-1}$), is almost 7000-fold faster at pH = 9.5 ($k_{obs} = 3.75$ $s^{-1}$), thus indicating that the reaction is catalyzed by $OH^-$ ions. From the slope of the log $k$ versus pH plot, the number of protons (1.7 ± 0.1) was determined. When the experiments with cathepsin B were performed in the same buffers but without NaCl, the inactivation rate constants were significantly diminished (Table 1).

The dependence of inactivation rate on temperature was studied with cathepsin B in the temperature range of 5−30 °C at pH = 8.0, using 50 mM Hepes buffer, containing 100 mM NaCl and 1 mM EDTA. The first-order rate constants were plotted against the inverse of absolute temperature, and an activation energy of 183.5 kJ $mol^{-1}$ was calculated from the slope of the Arrhenius plot (Figure 4).

*Effect of Dimethyl Sulfoxide.* The rate of inactivation was affected by the presence of organic solvent. The experiments were performed at pH 8.0 and 37 °C with increasing dimethyl sulfoxide concentrations [0.1−10% (v/v)] using 20 μM Z-Arg-Arg-AMC as substrate. As can be seen in Table 2, $k_{obs}$ increases almost twice between the two limits.

*Irreversibility of Cathepsin B Inactivation.* Cathepsin B was inactivated at pH 7.4. Its reactivation was then followed for 24 h at pH 6.0 and 37 °C, but no increase in catalytic activity was observed.

## DISCUSSION

Cysteine proteinases, including cathepsin B, are synthesized as inactive precursors, which are processed to the fully active form lacking the propeptide (Chan et al., 1986). In

Table 2: Effect of Organic Solvent Content on the Rate of Inactivation of Cathepsin B at pH 8.0 and 37 °C[a]

| % dimethyl sulfoxide (v/v) | $10^3 \times k_{obs}$ ($s^{-1}$) | % dimethyl sulfoxide (v/v) | $10^3 \times k_{obs}$ ($s^{-1}$) |
|---|---|---|---|
| 0.1 | 8.53 ± 1.01 | 7.5 | 14.61 ± 0.79 |
| 2.5 | 11.07 ± 1.17 | 10.0 | 15.68 ± 0.85 |
| 5.0 | 13.68 ± 1.19 | | |

[a] The experimental conditions are described in the Materials and Methods section. The best estimates for the observed inactivation rae constant $k_{obs}$ are given together with their standard errors and were calculated as described in the Results.

general, their activity is connected with the existence of an ion pair between the active-site Cys29 and His199 (Cys25 and His159 in papain). For their activity we might assume the following scheme (after Polgar, 1974):

$$-SH/^+HIm- \underset{}{\overset{pK_a = 3-4}{\rightleftharpoons}} -S^-/^+HIm- \overset{pK_a = 8-8.5}{\rightleftharpoons} -S^-/Im-$$

According to this scheme and others (Polgar, 1989; Polgar & Csoma, 1987; Brocklehurst, 1986), inactivation in alkaline media is caused by deprotonation of the imidazole moiety of the $-S^-/^+HIm-$ ion pair. This process is supposed to be reversible (see the above scheme). However, the pH-induced inactivation of cathespin B is shown to be an irreversible process, which is also in accordance with the previous results for cathepsins B (Barrett, 1973) and L (Turk et al., 1993a). Due to the irreversibility, we suggest the following mechanism for this process: deprotonation of His199, which is catalyzed by $OH^-$ ions, break the thiolate−imidazolium ion pair, which further influences ionization and solvent exposure of some charged residues. This then critically destabilizes the enzyme and leads to unfolding of the enzyme, which begins with conformational changes around the central α-helix region, where the active site Cys is located (Cys29 in cathepsin B), as is known from the crystal structures of the cysteine proteinases (Kamphuis et al., 1984; Baker, 1980; Musil et al., 1991). This hypothesis can be illustrated by the following scheme:

$$-SH/^+HIm- \overset{pK_a = 3-4}{\rightleftharpoons} -S^-/^+HIm- \overset{pK_a = 7-8.5}{\rightleftharpoons} -S^-/Im- \xrightarrow[k_{inac}]{k_{unf}} E^*$$

where $k_{inac}$ and $k_{unf}$ are the rate constants for inactivation and unfolding of the enzyme, respectively, and E* is the inactivated enzyme.

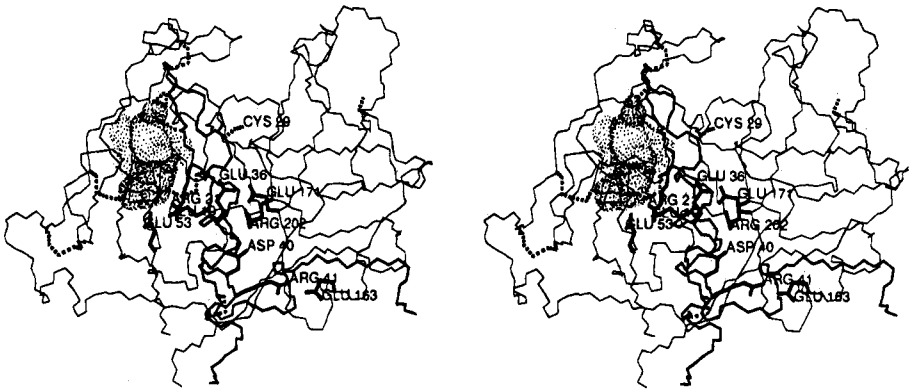


FIGURE 5: View along the interdomain interface of cathepsin B. The cathepsin B fold is shown with the main chain trace. The light chain including the central α-helix, on top of which the active site Cys29 is located, is shown with the line of medium thickness, the heavy chain with the thin line, and the side chains of the residues important for our explanation of protein stability are drawn with the thickest line. All these residues are also marked with their residue name and sequence number. Disulfide bridges are drawn with a dotted line. The dotted region on the left is a part of the Conoly surface of cathepsin B, which indicates a relatively deep solvent accessible cavity along the Arg21.

The measurements of circular dichroism of cathepsin B at pH = 5.5 and 7.4 clearly show the loss of the native structure, which indicates that cathepsin B inactivation is accompanied by a large conformational change. Similar observations were made with chicken cathepsin L, where inactivation was also accompanied by loss of the helix structure (Dufour et al., 1988). These results are in good agreement with the very high energy of activation of the inactivation process (183.5 kJ/mol), which is comparable to that (174.7 kJ/mol) found for cathepsin L (Turk et al., 1993a). Both values are also very close to that (195.0 kJ/mol) found for the alkaline-pH-induced unfolding of the staphylococcal nuclease (Chen et al., 1991).

The inactivation was found to be independent of the concentration of small, synthetic substrate as observed for rabbit cathepsin B (Baici & Knöpfel, 1986). By contrast, the inactivation rate was remarkably affected by the pH change. However, cathepsin B is substantially more stable than cathepsin L at neutral pH ($k_{inac} = 1.23 \times 10^{-3}$ s$^{-1}$ for cathepsin B, $k_{inac} = 0.254$ s$^{-1}$ for cathepsin L; Turk et al., 1993a; both at pH = 7.5 and 37 °C), as can be seen also from the slopes of log $k_{inac}$ versus pH plots (1.7 ± 0.1 for cathepsin B, 3.0 ± 0.1 for cathepsin L; Turk et al., 1993a). Similarly, the inactivation rate was also highly dependent on the ionic strength of the medium, and $k_{inac}$ increased almost 2-fold when ionic strength was increased for 0.1 M (Table 1). These two findings both indicate that ionic interactions are very important for the stability of cathepsin B, which will be discussed in more detail later on.

The pH-induced inactivation, as well as the unfolding of human cathepsin B, is shown to be a first-order process. The same was previously found for the pH-induced inactivation of rabbit cathepsin B (Baici & Knöpfel, 1986) and of human cathepsin L (Turk et al., 1993a). Moreover, the values of the inactivation rate constants and the unfolding rate constants obtained either from the circular dichroism measurements at 222 nm or from stopped-flow measurements of Trp fluorescence are similar (Table 1), indicating that pH-induced inactivation correlates also with protein stability and are also in agreement with other circular dichroism and temperature studies. The reactivation must be extremelyslow in comparison with the unfolding of the enzyme since no increase of the catalytic activity was observed even when the cysteine proteinase was exposed to alkaline conditions for a very short time (Turk et al., 1993a).

Since the crystal structure of cathepsin B (Musil et al., 1991) is known, we have tried to explain the irreversible pH-induced inactivation of this enzyme on structural grounds. As is known from the crystal structure of cathepsin B (Musil et al., 1991), the active site residues Cys29 and His199 are parts of two different domains. The active site is formed only when the two domains are held close together. As they separate, the central helix may unfold, as indicated by the circular dichroism experiments, and may prevent the reconstitution of the interdomain interface. Following this idea, we tried to localize the structural features that might destabilize the interdomain interface of cathepsin B with increasing pH and ionic strength of the medium. Our particular attention was directed toward the charged amino acid residues placed at the interdomain interface and the ones placed around the central α-helix on which the active site Cys29 resides.

The main chain connection of the two domains is shown in front (Figure 5); otherwise both domains are kept together by hydrogen bonding, electrostatic, and Van der Waals forces. Our first attention was directed to the line of charged residues (going from left to right in Figure 5): Glu19, Glu53, Glu36, and Arg21 and the two interdomain salt bridges Asp40−Arg202 and Arg41−Glu163. These residues anchor the central α-helix, at the beginning of which the active site Cys29 resides, to the rest of the molecule. The Glu19, Arg21, Glu36, and Arg202 resides are packed in a zipper fashion. At the opening of this zipper the pair Glu19 and Glu53 is situated. The closest interatomic distance between their two carboxylic oxygen atoms (2.86 Å) indicates that Glu19 and Glu53 share a proton. In the zipper region there are two relatively large cavities filled with solvent molecules. As can be seen in Figure 5, the first one, which is located between Glu19, Glu53, and Arg21, is accessible to the solvent (Figure 5). The second one (not shown in Figure 5 for clarity reasons) continues from Arg21 along Glu36 to the interdomain salt bridge Asp40−Arg202. The positions of the side chains of the residues Glu36 and Arg21 seem to be metastable: they are charged and buried inside the protein, but not involved in a salt bridge connection. An increased pH of the medium may repell the side chains of Glu19 and Glu53 from each other and thus increase the flexibility of the residues and solvent molecules along the zipper. This may lead to rearrangement of the side chains' packing along the zipper (via interchange of salt bridge partners) and

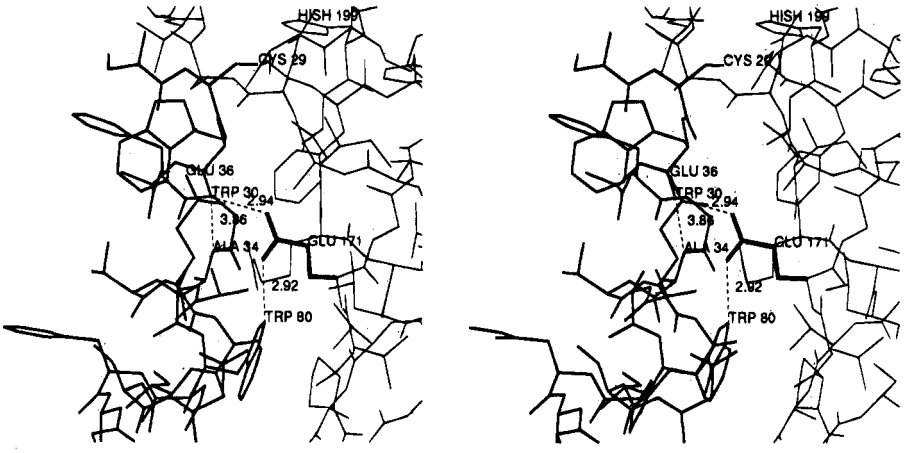


FIGURE 6: Placement of Glu171 into the interdomain interface of cathepsin B. For this plot the structure of human cathepsin B inhibited with an epoxy type of inhibitor (Turk, D., Podobnik, M., Popovič, T., Katunuma, N., Bode, W., Huber, R., & Turk, V., manuscript in preparation) was chosen because of the extreme O-Trp30−N-Ala34 distance (for comparison see Table 3). Parts of the left domain with the central α-helix are drawn with the line of a medium thickness, and parts of the right domain with a thin line, except the side chain of Glu171 (thick line). The distances listed in Table 3 are also shown.

Table 3: Interatomic Distances between Glu171 and the Related Amino Acid Residues in Different Structures of Papain, Actinidin, and Cathepsin B[a]

| | O-Trp30−N-Ala34 | O-Trp30−OE1-Glu171 | NE-Trp80−OE2-Glu171 |
|---|---|---|---|
| 9PAP | 3.11 | | |
| 1PAD | 3.20 | | |
| 1PPD | 3.09 | | |
| 2ACT | 3.09 | | |
| HCB1 | 3.72 | 3.19 | 3.19 |
| HCB2 | 3.62 | 2.81 | 3.07 |
| RCB1 | 3.62 | 2.78 | 2.99 |
| RCB2 | 3.72 | 2.77 | 2.96 |
| RCB3 | 3.81 | 2.84 | 3.05 |
| CBI1 | 3.86 | 2.94 | 2.92 |
| CBI2 | 3.55 | 2.66 | 3.01 |

[a] The interatomic distances related to Glu171 placement are shwon in Å. In the first column there are presented the distances between the two "helical" hydrogen-bonding atoms (carbonyl oxygen of Trp30 and the peptide bond nitrogen of Ala34-Trp26 and Ala30 in papain and actinidin sequences), in the second, the distances between the carbonyl oxygen of Trp30 and its nearest carboxylic group oxygen atom of Glu171, and in the third the distances between the hydrogen-bond-forming atoms of the other carboxylic group atom of Glu171 and NE of the Trp80. The distances listed in the second and the third columns have no equivalent in papain and actinidin structures. The papain (9PAP, Kamphuis et al., 1984; 1PAD, Drenth et al., 1976; 1PPD, Priestle et al., 1984) and actinidin (Baker, 1980) structures were taken from the Brookhaven Protein Data Bank. Human cathepsin B crystals contained two molecules (HCB1, HCB2, Musil et al., 1991; CBI1, CBI2, Turk, D., Podobnik, M., Popovič, T., Katunuma, N., Bode, W., Huber, R., & Turk, V., manuscript in preparation) per assymetric unit while rat cathepsin B crystals contained three (RCB1, RCB2, RCB3, Zučič, D., Musil, D., Turk, D., Engh, R. A., Katunuma, N., Turk, V., & Bode, W., manuscript in preparation).

destabilization of enzyme by opening the interdomain salt bridge Asp40−Arg202. Thus, this structural feature could result in the enzyme unfolding induced by the pH changes and increasing ionic strength of the medium. The indicated cavity (Figure 5) is not present in the papain structure (Kamphuis et al., 1984), which may contribute to the different pH stability profile of papain (Turk, B., Vučko, S., Turk, D., & Turk, V., manuscript in preparation).

Our second attention was directed toward Glu171, an acidic residue with no positive countercharge in its vicinity. As shown in Figure 6, its two carboxylic oxygen atoms are at hydrogen-bonding distance to the nitrogen of the Trp80 side chain and to the carbonyl oxygen of the Trp30 main chain, although the latter is supposed to be at a hydrogen-bonding distance with its corresponding peptide bond nitrogen atom of Ala34 at the next helical turn, as it is indeed in papain(Table 3). Our idea, based on the distance comparison of various available cathepsin B, papain, and actinidin structures (Table 3), is that the buried carboxylic group of Glu171 has a higher p$K$ value than is usual for Glu residues, so enabling the Glu171 to be protonated under nonbasic conditions. With increasing pH, however, it loses the proton and its interaction with the carbonyl oxygen of Trp30 turns from attractive to repulsive and so decreases the cathepsin B stability.

These suggest that cathepsin B is metastable and only the precursor can fold, forming the critical ionic interactions that remain to stabilize the enzyme in its active form. To possibly confirm these suggestions site-directed mutagenesis of cathepsin B shall be used. The mutation of Glu171 to Gln should increase the protein stability under alkaline conditions. Also the removal of a one of the two interdomain salt bridges should certainly destabilize cathepsin B (as already shown for Arg202 mutation by Hasnain et al., 1993). The role of the Glu53, Glu19, Arg21, and Glu36, however, seems to be more complicated. Its elucidation requires further studies on mutant structures.

In addition to the ionic interactions and hydrogen-bonding interactions, the hydrophobic interactions are also important for the stability of cathepsin B. The enzyme was found to be destabilized by dimethyl sulfoxide at pH 8.0. This solvent probably affects the internal hydrophobic interactions, which are important for the overall protein stability. Similar observations have already been made on rabbit cathepsin B

at pH 6.0 (Baici & Knöpfel, 1986). We suggest, therefore, that dimethyl sulfoxide concentrations above 1−2% (v/v) should be avoided in kinetic measurements of cathepsin B. These results are also in agreement with the studies on papain mutants, where it has been shown that the interdomain hydrophobic interactions were important for the thermostability of protein, probably due to stabilization of the central α-helix (Vernet et al., 1992).

## ACKNOWLEDGMENT

We thank Dr. Joseph G. Bieth, INSERM U392, Universite Louis Pasteur de Strasbourg, Illkirch, France; Dr. Ingemar Björk, Department of Veterinary Medical Chemistry, The Biomedical Center, Uppsala, Sweden; and Dr. Roger H. Pain, University Newcastle upon Tyne, UK, for the critical reading of the manuscript.

## REFERENCES

Aronson, N. N., & Barrett, A. J. (1978) *Biochem. J. 171*, 759−765.
Baici, A., & Knöpfel, M. (1986) *Int J. Cancer 38*, 753−761.
Baici, A., Lang, A., Hörler, D., & Knöpfel, M. (1988) *Ann. Rheumatic Dis. 47*, 684−691.
Bajkowski, A. S., & Frankfater, A. (1983a) *J. Biol. Chem. 258*, 1645−1649.
Bajkowski, A. S., & Frankfater, A. (1983b) *J. Biol. Chem. 258*, 1650−1655.
Baker, E. N. (1980) *J. Mol. Biol. 141*, 441−484.
Barrett, A. J. (1973) *Biochem. J. 131*, 809−822.
Barrett, A. J., & Kirschke, H. (1981) *Methods Enzymol. 80*, 535−561.
Bond, J. S., & Barrett, A. J. (1980) *Biochem. J. 189*, 17−25.
Cha, S. (1975) *Biochem. Pharmacol. 24*, 2177−2185.
Chan, S. J., San Segundo, B., McCormic, M. B., & Steiner, D. F. (1986) *Proc. Natl. Acad. Sci. U.S.A. 83*, 7721−7725.
Chen, H. M., You, J. L., Markin, V. S., & Tsong, T. Y. (1991) *J. Mol. Biol. 220*, 771−778.
Drenth, J., Kalk, K. H., & Swen, H. M. (1976) *Biochemistry 15*, 3731−3738.
Dufour, E., Dive, V., & Toma, F. (1988) *Biochim. Biophys. Acta 995*, 58−64.
Hasnain, S., Hirama, T., Tam, A., & Mort, J. S. (1992) *J. Biol. Chem. 267*, 4713−4721.
Hasnain, S., Hirama, T., Huber, C. P., Mason, P., & Mort, J. S. (1993) *J. Biol. Chem. 268*, 235−240.
Kamphuis, I. G., Kalk, K. H., Swarte, M. B. A., & Drenth, J. (1984) *J. Mol. Biol. 179*, 233−257.
Khan, M. Y., Agarwal, S. K., & Ahmad, S. (1992) *J. Biochem. (Tokyo) 111*, 732−735.
Khouri, H. E., Plouffe, C., Hasnain, S., Hirama, T., Storer, A. C., & Menard, R. (1991) *Biochem. J. 275*, 751−757.
Machleidt, W., Ritonja, A., Popovič, T., Kotnik, M., Brzin, J., Turk, V., Machleidt, I., & Müller-Esterl, W. (1986) in *Cysteine Proteinases and Their Inhibitors* (Turk, V., Ed.) pp 3−18, Walter de Gruyter, Berlin, New York.
Morrison, J. F., & Walsh, C. T. (1988) *Adv. Enzymol. Relat. Areas Mol. Biol. 61*, 201−301.
Mort, J. S., Recklies, A. D., & Poole, A. R. (1984) *Arthritis Rheum. 27*, 509−515.
Musil, D., Zučič, D., Turk, D., Engh, R. A. Mayr, I., Huber, R., Popovič, T., Turk, V., Towatari, T., Katunuma, N., & Bode, W. (1991) *EMBO J. 10*, 2321−2330.
Polgar, L. (1974) *FEBS Lett. 47*, 15−18.
Polgar, L. (1989) *Mechanisms of Protease Action*, CRC Press, Inc., Boca Raton, FL.
Polgar, L., & Csoma, C. (1987) *J. Biol. Chem. 262*, 14448−14453.
Priestle, J. P., Ford, G. C., Glor, M., Mehler, E. L., Smit, J. D. G., Thaller, C., & Jansonius, J. N. (1984) *Acta Crystallogr. A40*, Suppl. C-17.
Provencher, S. W. (1982) *Comput. Phys. Commun. 27*, 229−242.
Provencher, S. W., & Glöckner, J. (1981) *Biochemistry 20*, 33−37.
Rawlings, N. D., & Barrett, A. J. (1990) *CABIOS 6*, 118−119.
Ritonja, A., Popovič, T., Turk, V., Wiedenmann, K., & Machleidt, W. (1985) *FEBS Lett. 181*, 169−172.
Shaw, E. (1990) *Adv. Enzymol. Relat. Areas Mol. Biol. 63*, 271−347.
Sloane, B. F. (1990) *Semin. Cancer Biol. 1*, 137−152.
Sloane, B. F., Rozhin, J., Robinson, D. M., & Honn, K. V. (1990) *Biol. Chem. Hoppe-Seyler's 371* (Suppl.), 193−198.
Tian, W. X., & Tsou, C. L. (1982) *Biochemistry 21*, 1028−1032.
Turk, B., Dolenc, I., Turk, V., & Bieth, J. G. (1993a) *Biochemistry 32*, 375−380.
Turk, B., Križaj, I., Kralj, B., Dolenc, I., Popovič, T., Bieth, J. G., & Turk, V. (1993b) *J. Biol. Chem. 268*, 7323−7329.
Vernet, T., Tessier, D. C., Khouri, H. E., & Altschuh, D. (1992) *J. Mol. Biol. 224*, 501−509.
Willenbrock, F., & Brocklehurst, K. (1984) *Biochem. J. 222*, 805−814.
Willenbrock, F., & Brocklehurst, K. (1985a) *Biochem. J. 227*, 511−519.
Willenbrock, F., & Brocklehurst, K. (1985b) *Biochem. J. 227*, 521−528.
Willenbrock, F., & Brocklehurst, K. (1986) *Biochem. J. 238*, 103−107.
Zvonar, T., Kregar, I., & Turk, V. (1979) *Croat. Chem. Acta 52*, 411−416.